









Research Article

Optimization of CNC End Milling Process Parameters of Low-Carbon Mold Steel Using Response Surface Methodology and Grey Relational Analysis

R. Suresh Kumar ¹, **S. Senthil Kumar** ², **K. Murugan**,³ **B. Guruprasad** ⁴,
Sreekanth Manavalla ⁵, **S. Madhu** ⁶, **M. Hariprabhu** ⁷, **S. Balamuralitharan** ⁸,
and **S. Venkatesa Prabhu** ⁹

¹Department of Mechanical Engineering, Sri Eshwar College of Engineering, Coimbatore, India

²Department of Mechanical Engineering, RMK College of Engineering and Technology, Pudukottai, Tamil Nadu, India

³Government Polytechnic College, Valangaiman, Tamil Nadu, India

⁴Department of Mechanical Engineering, Alagappa Chettiar Government College of Engineering and Technology, Karaikudi, Tamil Nadu, India

⁵School of Mechanical Engineering & Electric Vehicles Incubation, Testing and Research Centre, Vellore Institute of Technology, Chennai, Tamil Nadu, India

⁶Department of Automobile Engineering, Saveetha School of Engineering, Saveetha Institute of Medical and Technical Sciences, Chennai, Tamil Nadu, India

⁷Department of Electrical and Electronics Engineering, M. Kumarasamy College of Engineering, Karur, Tamil Nadu, India

⁸Department of Mathematics, College of Engineering and Technology, SRM Institute of Science and Technology, Kattankulathur, Chengalpattu, Tamil Nadu, India

⁹Department of Chemical Engineering, College of Biological and Chemical Engineering, Addis Ababa Science and Technology University, Addis Ababa, Ethiopia

Correspondence should be addressed to R. Suresh Kumar; rsk777mech@gmail.com and S. Venkatesa Prabhu; venkatesa.prabhu@aastu.edu.et

Received 15 June 2021; Revised 29 June 2021; Accepted 3 August 2021; Published 16 August 2021

Academic Editor: Antonio Gloria

Copyright © 2021 R. Suresh Kumar et al. This is an open access article distributed under the Creative Commons Attribution License, which permits unrestricted use, distribution, and reproduction in any medium, provided the original work is properly cited.

The manufacturing sectors are consistently striving to figure out ways to minimize the consumption of natural resources through rational utilization. This is achieved by a proper understanding of every minute influence of parameters on the entire process. Understanding the influencing parameters in determining the machining process efficacy is inevitable. Technological advancement has drastically improved the machining process through various means by providing better quality products with minimum machining cost and energy consumption. Specifically, the machining factors such as cutting speed, spindle speed, depth of cut, rate of feed, and coolant flow rate are found to be the governing factors in determining the economy of the machining process. This study is focused on improving the machining economy by enhancing the surface integrity and tool life with minimum resources. The study is carried out on low-carbon mold steel (UNS T51620) using Box–Behnken design and grey regression analysis. The optimized multiobjective solution for surface roughness (R_a), material removal rate (MRR), and power consumed (P_c) and tool life is determined and validated through the confirmatory run. The optimized set of parameters in Box–Behnken design and grey regression analysis with that of confirmatory runs shows a 10% deviation that proves the reliability of the optimization techniques employed.

1. Introduction

In the past decades, CNC machining has gained an irreplaceable stand in offering higher reliability, accuracy, and productivity. Moreover, CNC milling provides higher flexibility in choosing the machining parameters levels when compared to a conventional milling process. In industries, different types of milling processes are employed such as plain milling, end milling, side milling, and gang milling. Out of these, in automobile, aerospace, and metal processing industries, the CNC end milling process is inevitable due to its high precision accuracy and reliability. Being a versatile process, end milling has already conquered unrivalled place in the manufacturing sector fulfilling the requirements. In any machining process, numerous parameters are involved that govern the process. These parameters are classified as controllable and noncontrollable parameters. Controllable parameters are those which can be tuned according to the needs such as spindle rotation, cutting wheel speed, rake angle, feed rate, and depth of cut. Noncontrollable parameters are those which cannot be directly controlled rather can be governed indirectly through controllable parameters. Tool wear, surface roughness, and chip formation vibrations are few to name.

An experimental study was carried on Al2014-T6 by Ming-Yung and Chang [1] on surface integrity. Trial runs were conducted by slot end milling. The study revealed that vibrations during machining and the rate of feed are the key factors governing the surface roughness. Palanisamy et al. [2] explored the machining consequences for CNC end milling and arrived at an optimized set of machining parameters. The study included application of a genetic algorithm, and the result revealed a higher influential contribution by feed and depth of cut on surface roughness. A detailed study on the implementation of adaptive control in CNC machining was carried out by Suresh Kumar et al. [3]. In this study, the research progress in maintaining the accuracy and reliability of machining parameters was discussed elaborately. The article summed up the techniques developed so far in improving the efficacy of CNC machining. A theoretical approach was proposed for forecasting surface integrity by Martellotti [4] and Quintana et al. [5]. The study was restricted to a single-objective function where the possible effects of other responses were not considered. An analytical model was developed by Mansour and Abdalla [6]. A comparison study was presented by Suresh Kumar et al. [7], which focused on deviation recorded between genetic algorithm (GA) and artificial neural networks (ANN) in achieving optimum machining factors for CNC milling.

Alauddin et al. [8] investigated controllable factors affecting the roughness and life of the tool used for machining. Cutting speed, rate of feed, and depth of axial cut are taken as the governing parameters. Chang et al. [9] and Coker and Shin [10] conceded the optimization exploration using DOE on face roughness. In another research, DOE was used by Gologlu and Sakarya [11] and Dhokia et al. [12] to predict the optimum level of surface roughness. Suresh Kumar et al. [13] optimized CNC end milling of BSL168 using Box-Behnken design. The material considered was an

aluminium composite used for aeronautical applications. The work included optimization of contradictory responses, namely surface integrity and MRR by controlling the machining constraints namely spindle speed, rate of feed, and depth of cut.

The literature survey also provides an insight into the application of advanced optimization techniques such as GA, ANN, and fuzzy [14–19] to arrive at an optimized set of parameters for machining. Kumar et al. [20] investigated the influencing parameters in the machining of AMS 4205. The experiment involved a multiobjective approach towards providing a solution for achieving optimum results for roughness and MRR. The study included Taguchi robust design and Box-Behnken design for arriving at the optimized level of parameters. A detailed literature survey was carried out by Zain et al. [21] on genetic algorithm and their application towards the optimization of cutting parameters in CNC milling. Suresh Kumar et al. [22] optimized the surface integrity using CNC milling. The material considered was A91060 and HSS tools used. The study included the application of response surface methodology to derive the governing mathematical model for finding the optimum solution through genetic algorithms.

A detailed report on the machining effect between the work material and tool used was carried out by Brezocnik and Kovacic [23]. Ganesh Kumar et al. [24] carried out a detailed review on cutting tool measurement in the turning process using cloud computing systems. The study involved the application of a genetic algorithm limited to a single objective function. Oktem et al. [25] applied a genetic algorithm in arriving at the optimized parameter to achieve minimum surface roughness. A multiobjective approach for optimization of cyclone separator was carried out by Venkatesh et al. [26] using Taguchi robust design and validated using numerical simulation. Ganesh Kumar et al. [27] suggested optimum tool stress in CNC turning of EN8 steel using a numerical approach.

From the above-detailed study, one can witness extensive research in the field of machining processes using higher-order optimization tools. At the same time, it is noteworthy to state that most of the work executed is limited to single-objective functions. In reality, any machining process is always associated with more than one response of contradictory nature. Therefore, it becomes obligatory to cram the consequences of accompanying responses to fix the preeminent machining parameters.

This study addresses a multiobjective function where an attempt is made to arrive at optimizing contradictory responses namely roughness (R_a), MRR, and power consumption (P_c). The work material is a low-carbon mold steel (UNS T51620), which is hard to machine.

2. Experimental Outline

The sequential approach of the study is given as follows:

- (1) Assigning of levels for each parameter
- (2) Execution of experimental run based on Box-Behnken design

- (3) Measurement of the roughness, MRR, and tool life in terms of P_c
- (4) Development of mathematical model for the prediction of R_a , MRR, and P_c . It is also subjected to adequacy check using ANOVA
- (5) Application of grey regression analysis (GRA) for optimization
- (6) Confirmatory runs to validate the results attained

3. Methodology and Implementation

3.1. Material and Tool. Low-carbon mold steels contain chromium and nickel as the main alloying elements and are classified in group P steels. These steels are usually nitrided or carburized to attain the desirable qualities. These steels are good in machinability as they can be easily machined into complex and large molds and dies. They are mostly used in injection molds and die casting. Due to its wide range of applications, prehardened UNS T51620 steel is taken as the work material. The material hardness ranges between 30 and 40 HRC. Rectangular work material of dimensions 75 mm × 30 mm × 12 mm is taken for machining. The elemental composition of the material is shown in Table 1. The material is found to have extensive applications in electronic equipment, car accessories, and home appliances.

The work material is hard in nature due to the presence of manganese and nickel in higher percentages followed by carbon content as stated in Table 1. Based on the literature survey, TiCN is taken as the cutting tool material having a Rockwell hardness of 88.

3.2. Controllable and Noncontrollable Parameters. A machining operation is highly influenced by parameters such as speed of spindle, feed, depth of cut, tool rake angle, coolant flow rate, roughness, and tool life. Out of these, certain parameters can be governed before the execution of machining, and they are known as controllable parameters, whereas certain parameters vary based on the influence of so-called controllable parameters. Such dependent parameters are known as noncontrollable factors. In this study, the controllable factors are speed of the spindle (A), depth of cut (B), feed (C), and flow rate of coolant (D). The noncontrollable factors or responses are taken as surface roughness (R_a), material removal rate (MRR), and power consumed (P_c). The levels of the selected controllable parameters are finalized based on the manufacturer's specifications and researches carried out so far.

The controllable parameters identified are feed (mm/min), spindle speed (rpm), depth of cut (mm), and flow rate of coolant (l/min). Figure 1 shows the trial runs conducted in a 3-axis vertical milling centre. A surface tester (Mitutoyo) is employed for measuring the roughness of the machined. Figure 2 shows the experimental runs conducted on the work material. The surface tester has a resolution varying from 0.01 microns to 0.3 microns. The average roughness value (R_a) is considered for the analysis.

TABLE 1: Chemical composition.

Mn	Cr	Ni	C	Si	Mo	S
0.86	0.033	0.8	0.36	0.44	0.9	0.35



FIGURE 1: Trial runs conducted.



FIGURE 2: Measurement of roughness.

3.3. Design Matrix. Experimental iterations were based on Box-Behnken model. The controllable parameters are assigned with three levels, and two responses are considered as detailed in Table 2. The sequence of experimental runs and responses are shown in Table 3.

4. Results and Discussions

The parametric effects on the responses are discussed individually in the following sections. For each response, optimized level of machining parameters based on desirability function. The competency of the desirability function is validated by analysis of variance (ANOVA).

4.1. Response Surface Model for the Prediction of Surface Roughness. The ANOVA analysis for roughness (R_a) is given in Table 4.

" F -value" of 636600 with " P value" below 0.0001 confirms the significance of the desirability function. The function is said to be insignificant if the values are greater than 0.10. In other words, a 0.01% chance is there that an

TABLE 2: Machining parameters and their levels.

Parameters	Unit	Level 1	Level 2	Level 3
Spindle speed (<i>A</i>)	rpm	1200	1850	2500
Depth of cut (<i>B</i>)	mm	0.2	0.4	0.6
Feed rate (<i>C</i>)	mm/min	1000	1500	2000
Coolant flow rate (<i>D</i>)	l/min	4	6	8

TABLE 3: Experimental runs and responses.

<i>A</i> (rpm)	<i>B</i> (mm)	<i>C</i> (mm/min)	<i>D</i> (l/min)	R_a (microns)	MRR (mm ³ /min)	P_c (HP)
1850	0.2	1000	6	4.217	0.2361	0.207
1850	0.6	2000	6	2.650	1.2931	1.408
1200	0.4	1000	6	4.797	0.7826	0.751
2500	0.4	2000	6	2.070	0.7466	0.865
2500	0.4	1500	4	2.746	0.6249	0.635
1200	0.4	2000	6	4.550	0.8636	1.026
1850	0.4	1500	6	3.434	0.7646	0.808
1850	0.2	1500	4	4.646	0.1954	0.253
1850	0.4	1500	6	3.434	0.7646	0.808
1850	0.4	1500	6	3.434	0.7646	0.808
1200	0.2	1500	6	5.334	0.3351	0.425
2500	0.4	1500	8	1.642	0.7873	0.819
1850	0.2	1500	8	3.542	0.3578	0.437
2500	0.6	1500	6	1.534	1.1941	1.190
1200	0.4	1500	8	4.122	0.9043	0.981
1850	0.6	1000	6	2.897	1.2121	1.133
1850	0.4	1000	4	4.109	0.6429	0.578
1850	0.4	2000	8	2.758	0.8863	1.037
1850	0.4	1000	8	3.005	0.8053	0.762
1200	0.6	1500	6	4.014	1.3111	1.351
1200	0.4	1500	4	5.226	0.7419	0.796
2500	0.2	1500	6	2.854	0.2181	0.264
1850	0.6	1500	8	2.222	1.3338	1.363
1850	0.2	2000	6	3.970	0.3171	0.482
1850	0.4	1500	6	3.434	0.7646	0.808
1850	0.6	1500	4	3.326	1.1714	1.179
1850	0.4	1500	6	3.434	0.7646	0.808
1850	0.4	2000	4	3.862	0.7239	0.853
2500	0.4	1000	6	2.317	0.6656	0.590

TABLE 4: Roughness (R_a)—analysis of variance.

Response surface linear model						
Analysis of variance						
Source	Sum of squares	df	Mean square	<i>F</i> -value	<i>P</i> value	
Model	27.52382748	4	6.88095687	636600.00	<0.0001	Significant
<i>A</i>	18.45715248	1	18.45715248	628620.00	<0.0001	
<i>B</i>	5.2272	1	5.2272	68590	<0.0001	
<i>C</i>	0.183027	1	0.183027	5998618.94	<0.0001	
<i>D</i>	3.656448	1	3.656448	1834573.15	<0.0001	
Residual error	1.58333	24	0			
Lack of fit	0	20	0			
Pure error	0	4	0			
Cor total	27.52382748	28				
Standard deviation	0.000397911		R^2	0.999998975		
Mean	0.54264		Adj R^2	0.99999754		
CV (%)	0.073328765		Pred R^2	NA		
PRESS	NA		Adequate precision	3152.502951		

insignificant effect may arise due to noise. Moreover, R^2 , Adj R^2 , and Pred R^2 values indicate a positive approach towards its higher efficacy, and the values are close to 1. The surface interaction plots shown below provide a lucid view on the interaction between machining parameters and the response R_a .

4.1.1. Parameter Interaction Effects. The interaction graph for parameters A and B on response R_a is shown in Figure 3. Minimum roughness is achieved when spindle speed is at its maximum level of 2500 rpm with feed rate maintained at its intermediate level of 1500 mm/min. Any deviation from the above-mentioned level resulted in an adverse effect on response R_a . It is noteworthy to observe that parameter B provides a flexible range between 0.4 mm and 0.6 mm. The interaction graph for D and C on response R_a is depicted in Figure 4. The effect of parameter D is found to have the least contribution on R_a when measured with supplementary parameters considered.

Figure 5 shows the interaction graph of parameters A and D on R_a . When the level of parameter D is maintained between 4 l/min to 8 l/min, it resulted in achieving minimum surface roughness but is found to be associated with the influence of spindle speed. Better results are attained when parameter A is increased gradually along with parameter D.

The effect of parameters C and D is depicted in Figure 6. On careful analysis, one can find that parameter C dominates over parameter B influencing the response R_a . From experimental runs 3 and 6, one can find that increasing the level of feed rate minimizes the roughness. At the same time, experimental run 28 exhibits the influence of parameter A on surface roughness when the other parameters are kept at the same level as stated in runs 3 and 6. This provides a lucid view on the influencing parameters affecting the response R_a . In this case, the order of prominent parameters influencing the response R_a is in the order of parameters A and C followed by parameters B and D.

4.1.2. Predicted Optimum Parameters for R_a . Table 5 shows the optimized level of machining parameters.

4.2. Response Surface Model for the Prediction of MRR. The ANOVA analysis for the response MRR is highlighted in Table 6. “F-value” of 668091 with “P-value” below 0.0001 shows the significance of the developed model. The function is said to be insignificant if the values are greater than 0.10. In other words, a 0.01% chance is there that an insignificant effect may arise due to noise. Moreover, R^2 , Adj R^2 , and Pred R^2 values indicates a positive approach towards its higher efficacy as the values are close to 1. The surface interaction plots shown below provide a lucid view on the interaction between machining parameters and the response MRR.

4.2.1. Parameter Interaction Effects. The following interaction graph depicts the effect of the parameters on MRR. Figure 7 reflects the interaction effect of parameters A and B on MRR. Experimental runs 1, 16, and 17 show a gradual

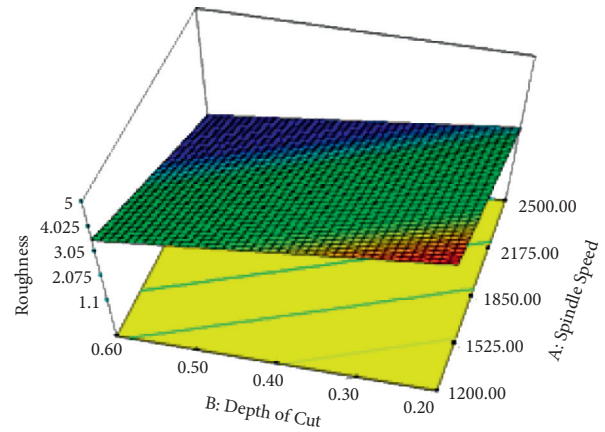


FIGURE 3: Interaction graph of A and B on R_a .

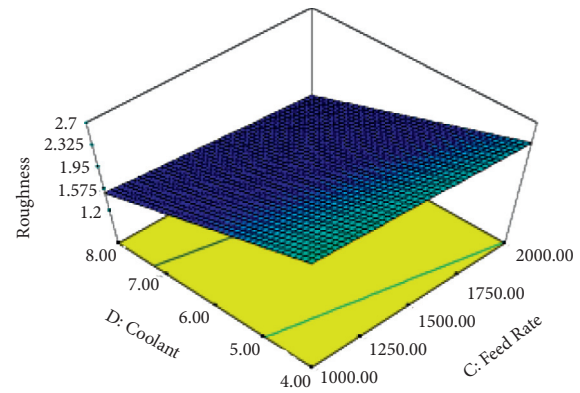


FIGURE 4: Interaction graph of C and D on R_a .

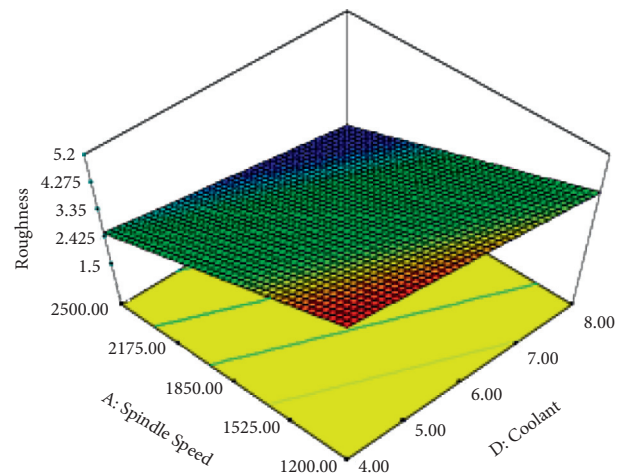


FIGURE 5: Interaction graph of A and D on R_a .

increase in MRR when parameters A and C are kept at level 1 and parameter C is gradually increased. On the other hand, in experimental runs 5, 11, and 13, the level of parameter A is changed, and other parameters are assigned at level 1. It is observed that though there is an increase in MRR, the rate of

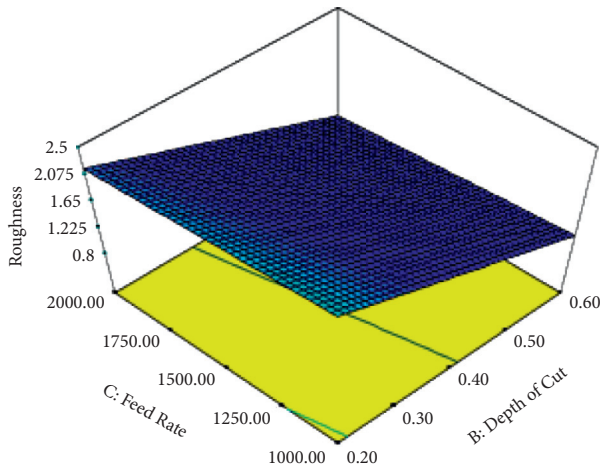


FIGURE 6: Interaction graph of C and D on R_a .

TABLE 5: Optimized level of parameters for roughness.

A (rpm)	B (mm)	C (mm/min)	D (l/min)	R_a (microns)
2495.75	0.47	1000.01	8	1.5439

increase seen is much lower than in the former case. This evidence established firmly that parameter C plays a very prominent role compared to parameter A.

The machining effect of parameters C and B on MRR is shown in Figure 8. Experimental runs 4, 5, and 29 show a gradual increase in MRR when parameters A and B are maintained at 2500 rpm, 0.4 mm, respectively, and parameter C is gradually increased. Whereas, in experimental runs 8, 9, and 26, the level of parameters A and C are kept constant (1850 rpm and 1500 mm/min), and parameter B is varied. It is observed that there is a drastic increase in MRR when compared with that of parameter C. This evidence established firmly that parameter B plays a very prominent role compared to parameter C.

Figure 9 describes the machining effect of parameters D and C on MRR. Experimental runs 8 and 13, 18 and 28, and 23 and 26 clearly depict the effect of parameter D when other parameters are kept constant. In the above-stated experimental runs, a pattern of increase in MRR can be observed. The applied coolant enhances the quantity of material removed by washing off the removed materials and heat generated while machining. On the other hand, in experimental runs 3 and 6 and runs 17 and 28, the level of parameter C is alone changed and found that the application of coolant enhances MRR compared to parameter C but depends on parameters B and A.

The machining effect of parameters A and D on MRR is shown in Figure 10. Experimental runs 8 and 13, 18 and 28, and 23 and 26 clearly depict the effect of coolant flow rate when other parameters are kept constant. In the above-stated experimental runs, an increase in the MRR is observed. On the other hand, experimental runs 11 and 22, 3 and 29, and 14 and 20 show an increase in MRR when spindle speed is varied keeping all other parameters constant.

4.2.2. Predicted Optimized Set of Machining Parameters for MRR. Table 7 shows the optimized level of machining parameters.

4.3. Response Surface Model for the Prediction of Power Consumed (P_c). Table 8 reflects the ANOVA analysis for the response, P_c . “F-value” of 534600.00 with “P-value” below 0.0001 highlights the significance of the developed function. The function is said to be insignificant if the values are greater than 0.10. In other words, a 0.01% chance is there that an insignificant effect may arise due to noise. Moreover, R^2 , Adj R^2 , and Pred R^2 values indicate a positive approach towards its higher efficacy as the values are close to 1. The interaction graphs shown below provide a lucid view on the interaction between machining parameters and the response P_c .

4.3.1. Parameter Interaction Effects. Figures 11 and 12 interpret the interaction effect of machining parameters on power consumption (P_c). Figure 11 reflects the machining effect of parameters A and B on P_c . Experimental runs 8 and 9, 12 and 22, and 11 and 15 show a rapid increase in power consumption when feed rate is increased, while other parameters are taken as constant. This shows that an increased parameter B increases the force of cutting, thereby consuming more power. On the other hand, in experimental runs 12, 15, and 17 when the level of parameter A is changed and other parameters are kept constant, an increase in power consumption is observed as parameter A increases. But the impact on power consumption is a little lower when compared to parameter B.

Figure 12 reflects the effect of parameters B and C on power consumption. Experimental runs 4, 5, and 29 show a rapid increase in power consumption when parameter C is increased while other parameters are taken as constant. This indicates that an increase in parameter C considerably increases power consumption due to drastic variations in cutting forces. On the other hand, in experimental runs 8, 9, and 26 parameter A is changed, and other parameters are assigned as constant. From the experimental runs, it is observed that though parameter A affects power consumption directly, it is highly influenced parameter B followed by C.

In Figure 13, the machining behaviour of parameters D and C on P_c is shown. Experimental runs 8 and 13, 18 and 28, and 23 and 26 clearly depict the effect of parameter D when other parameters are kept constant. In the above-stated experimental runs, an increase in power consumption is observed in the above-mentioned runs. This proves that coolant contributes negligibly in addressing power consumption. On the other hand, in experimental runs 3 and 6 and runs 17 and 28, the level of parameter C is alone changed and is observed that an increase in parameter C on P_c .

Figure 14 represents the machining effect of parameters A and D and coolant on P_c . Experimental runs 8 and 13, 18 and 28, and 23 and 26 clearly depict the effect of parameter D when other parameters are kept constant. In the above-stated experimental runs, it is observed that coolant

TABLE 6: Material removal rate (MRR)—analysis of variance.

Response surface linear model						
Analysis of variance table						
Source	Sum of squares	df	Mean square	F-value	P value	
Model	2.99759928	4	0.74939982	668091.1902	<0.0001	Significant
A	0.041067	1	0.041067	1034328.952	<0.0001	
B	2.857728	1	2.857728	749879.2755	<0.0001	
C	0.019683	1	0.019683	430180.4257	<0.0001	
D	0.07912128	1	0.07912128	636600.00	<0.0001	
Residual error	1.87633	24	0			
Lack of fit	0	20	0			
Pure error	0	4	0			
Cor total	2.99759928	28				
Standard deviation	0.000697911		R^2	0.98768975		
Mean	0.54264		Adj R^2	0.98524754		
CV (%)	0.073328765		Pred R^2	NA		
PRESS	NA		Adequate precision	2152.502951		

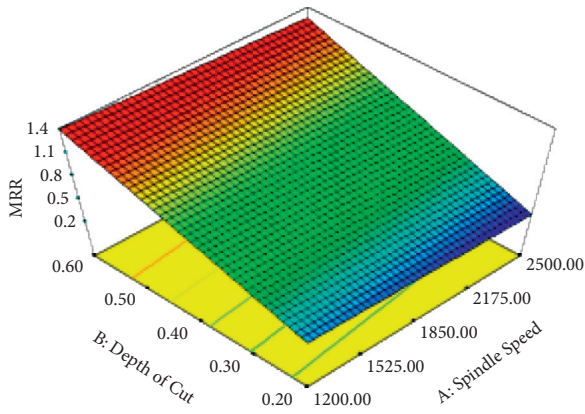


FIGURE 7: Interaction graph of B and A on MRR.

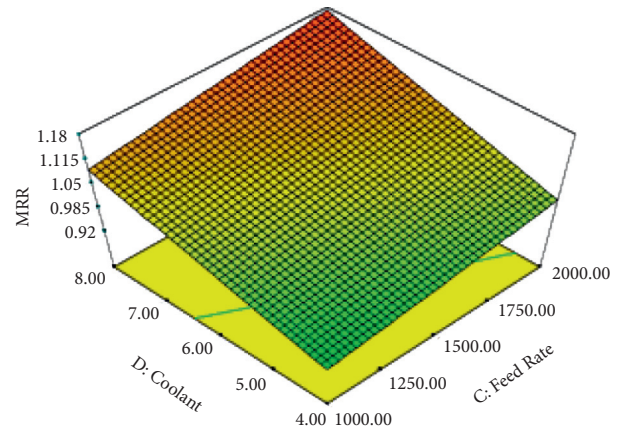


FIGURE 9: Interaction graph of D and C on MRR.

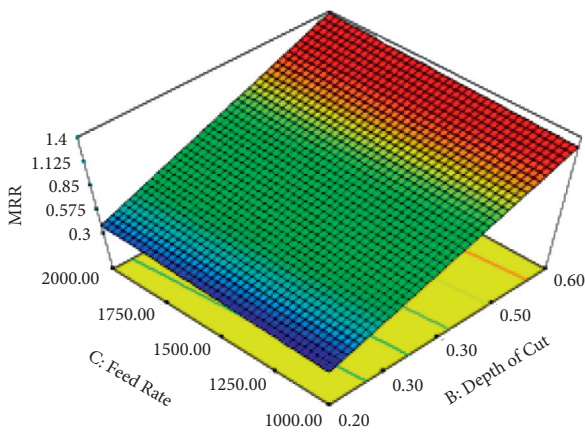


FIGURE 8: Interaction graph of C and B on MRR.

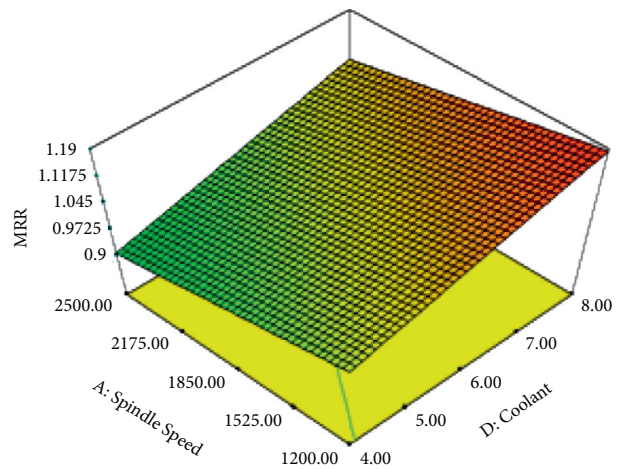


FIGURE 10: Interaction graph of A and D on MRR.

behaviour varies depending upon the combination of other parameters. On the other hand, experimental runs 11 and 22, 3 and 29, and 14 and 20 show a decrease in P_c when parameter A is increased.

4.3.2. Predicted Optimized Set of Machining Parameters for P_c . Table 9 shows the optimized level of machining parameters.

TABLE 7: Optimized level of parameters for MRR.

A (rpm)	B (mm)	C (mm/min)	D (l/min)	MRR (IPM)
2495.75	0.47	1000.01	8	0.916658

TABLE 8: Power consumed (P_c)—ANOVA.

Source	Sum of squares	df	Analysis of variance			P value	Significant
			Mean square	F-value			
Model	2.9792694	4	0.74481735	534600.00	<0.0001		
A	0.07795632	1	0.07795632	512366.00	<0.0001		
B	2.572428	1	2.572428	636600.00	<0.0001		
C	0.226875	1	0.226875	506366.00	<0.0001		
D	0.10201008	1	0.10201008	47690.00	<0.0001		
Residual error	3.87633	24	0				
Lack of fit	0	20	0				
Pure error	0	4	0				
Cor total	2.9792694	28					
Standard deviation	0.000786511		R^2	0.98557689			
Mean	0.57264		Adj R^2	0.95952475			
CV (%)	0.083328765		Pred R^2	NA			
PRESS	NA		Adequate precision	3152.502951			

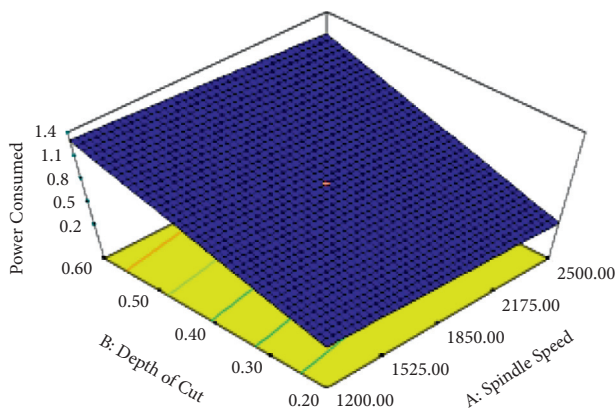


FIGURE 11: Interaction graph of A and C on P_c .

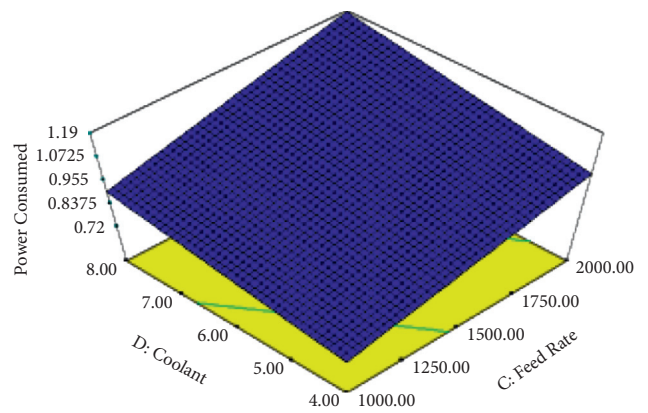


FIGURE 13: Interaction graph of D and C on P_c .

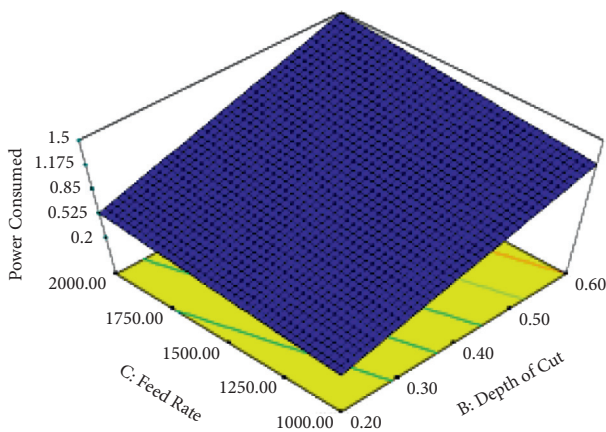


FIGURE 12: Interaction graph of C and B on P_c .

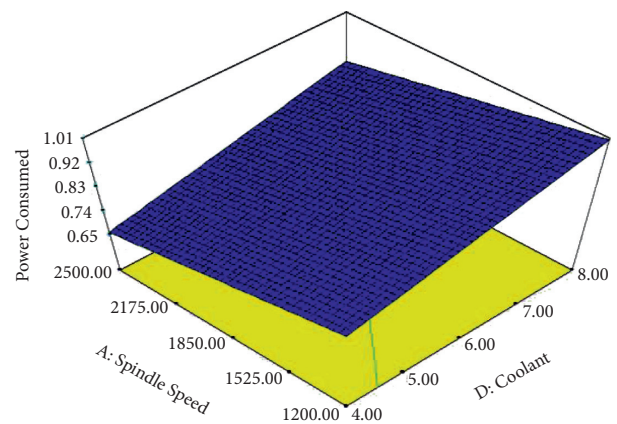


FIGURE 14: Interaction graph of A and D on P_c .

TABLE 9: Optimized level of parameters for power consumption (P_c).

A (rpm)	B (mm)	C (mm/min)	D (l/min)	P_c (HP)
2495.75	0.47	1000.01	8	0.843122

TABLE 10: Grey regression analysis.

Normalized values			Deviation sequence			Grey relation coefficients			Grey relational grade	Rank
R_a	P_c	MRR	R_a	P_c	MRR	R_a	P_c	MRR		
0.294	1.000	0.976	0.706	0.000	0.024	0.415	1.000	0.954	0.790	2
0.706	0.000	0.096	0.294	1.000	0.904	0.630	0.333	0.356	0.440	26
0.141	0.547	0.521	0.859	0.453	0.479	0.368	0.525	0.511	0.468	22
0.859	0.453	0.551	0.141	0.547	0.449	0.780	0.477	0.527	0.595	10
0.681	0.644	0.652	0.319	0.356	0.348	0.611	0.584	0.590	0.595	9
0.206	0.318	0.453	0.794	0.682	0.547	0.386	0.423	0.478	0.429	27
0.500	0.500	0.536	0.500	0.500	0.464	0.500	0.500	0.519	0.506	14
0.181	0.962	1.010	0.819	0.038	-0.010	0.379	0.930	1.020	0.776	3
0.500	0.500	0.536	0.500	0.500	0.464	0.500	0.500	0.519	0.506	14
0.500	0.500	0.536	0.500	0.500	0.464	0.500	0.500	0.519	0.506	14
0.000	0.818	0.894	1.000	0.182	0.106	0.333	0.734	0.824	0.630	7
0.972	0.490	0.517	0.028	0.510	0.483	0.946	0.495	0.509	0.650	6
0.472	0.809	0.875	0.528	0.191	0.125	0.486	0.723	0.799	0.670	4
1.000	0.182	0.178	0.000	0.818	0.822	1.000	0.379	0.378	0.586	11
0.319	0.356	0.420	0.681	0.644	0.580	0.423	0.437	0.463	0.441	25
0.641	0.229	0.163	0.359	0.771	0.837	0.582	0.393	0.374	0.450	24
0.322	0.691	0.637	0.678	0.309	0.363	0.425	0.618	0.580	0.541	12
0.678	0.309	0.435	0.322	0.691	0.565	0.608	0.420	0.469	0.499	19
0.613	0.538	0.502	0.387	0.462	0.498	0.564	0.520	0.501	0.528	13
0.347	0.047	0.081	0.653	0.953	0.919	0.434	0.344	0.352	0.377	29
0.028	0.510	0.555	0.972	0.490	0.445	0.340	0.505	0.529	0.458	23
0.653	0.953	0.991	0.347	0.047	0.009	0.590	0.913	0.982	0.829	1
0.819	0.038	0.062	0.181	0.962	0.938	0.734	0.342	0.348	0.475	21
0.359	0.771	0.908	0.641	0.229	0.092	0.438	0.686	0.845	0.656	5
0.500	0.500	0.536	0.500	0.500	0.464	0.500	0.500	0.519	0.506	14
0.528	0.191	0.197	0.472	0.809	0.803	0.515	0.382	0.384	0.427	28
0.500	0.500	0.536	0.500	0.500	0.464	0.500	0.500	0.519	0.506	14
0.387	0.462	0.570	0.613	0.538	0.430	0.449	0.482	0.538	0.490	20
0.794	0.682	0.618	0.206	0.318	0.382	0.708	0.611	0.567	0.629	8

5. Optimization of Parameters by Grey Regression Analysis

The following steps are followed to arrive at the optimal solutions:

- (1) Normalization of responses: in this step, preprocessing of data is performed based on the objective function defined. If the normalization or data preprocessing is based on the "larger the better" function, then it is computed based on equation (1). If the normalization or data preprocessing is based on "smaller the better" function, then it is computed based on equation (2). Normalization is a method to arrive at a comparable data set from the original set of data reducing the percentage of variation for ease of analysis.

$$Xi(k) = \frac{xi(k) - \min xi(k)}{\max xi(k) - \min xi(k)}, \quad (1)$$

$$Xi(k) = \frac{\max xi(k) - xi(k)}{\max xi(k) - \min xi(k)}, \quad (2)$$

where $i = 1, \dots, m$, $k = 1, \dots, n$, m is the number of experimental data, and n is the number of responses. $Xi(k)$ represents the value after data preprocessing; $xi(k)$ represents the original sequence data; $\max xi(k)$ is the largest value of $xi(k)$; and $\min xi(k)$ is the minimal value.

- (2) Computation of deviation sequence: based on responses, "smaller the better" option is applied for R_a and P_c whereas for MRR, the "larger the better" option is applied. In this step, the deviation is calculated for normalized values. In this, for each response, the deviation in each case is recorded with respect to the higher normalized value attained.
- (3) Computation of grey relational coefficients: the grey regression coefficients are calculated using the relation shown in equation (3): Here, $\xi_i(k)$ is the grey relational coefficient. Δ_{\min} and Δ_{\max} are the minimum and maximum values of absolute differences. And, ψ is 0.5, which is the distinguishing or identification coefficient that usually ranges from 0 to 1:

TABLE 11: Optimized parameter by GRA.

A (rpm)	B (mm)	C (mm/min)	D (l/min)
2500	0.2	1500	6

TABLE 12: Confirmatory runs.

Optimization tool	A (rpm)	B (mm)	C (mm/min)	D (l/min)	R_a (microns)	MRR (IPM)	P_c (HP)
Box-Behnken	2495.75	0.47	1000.01	8	1.543	0.916658	0.843122
GRA	2500	0.2	1500	6	1.398	0.8296	0.7961
Deviation					0.154	0.087	0.047
% deviation					10	9	6

$$\xi_i(k) = \frac{\Delta \min + \psi \Delta \max}{\Delta o_i(k) + \psi \Delta \max} \quad (3)$$

- (4) Computation of grey relational grade: the grey relational grade (γ) represents the correlation level between the reference and comparability sequences. In this stage, a multiobjective function is converted into a single-objective function. The following equation is the governing equation for arriving at grey relational grade:

$$\gamma^i = \frac{1}{n} \sum_{k=1}^n \xi_i(k). \quad (4)$$

- (5) Optimal parameters: in this step, rank is identified for each set of values. Based on the rank attained, the optimized level is easily figured out which provides the optimum solution by considering all responses together.

Table 10 shows the grey regression analysis performed on the experimental values.

5.1. Optimized Set of Parameters Using Grey Regression Analysis (GRA). From Table 10, the highest rank is contributed by the 22nd experimental run, which includes the following combination of parameters (Table 11).

6. Confirmatory Runs

To validate the above, confirmatory runs were conducted, and Table 12 shows the results attained.

7. Conclusions

The machining parameter optimization is performed on the low-carbon mold steel in CNC end milling. The responses roughness, MRR, power consumption, and tool life were optimized. The optimization process includes responses that have contradictory effect on each other. For example, the objective function needs to be minimum for optimizing roughness and power to arrive at minimum machining cost. At the same time, the production time taken must also be

minimum where the material removal rate comes into play. The objective function for material removal rate is always maximum, which is opposite to the previous one. Therefore, the process becomes complex, and to arrive at the optimal solution, one has to approach a multiobjective function. In this experimental analysis, the following observations are found to be notable:

- (1) Minimum surface roughness attained in the combination of 2500 rpm, 0.6 mm, 1500 mm/min, and 6 l/min
- (2) Minimum power consumption attained in the combination of 1850 rpm, 0.2 mm, 1000 mm/min, and 6 l/min
- (3) Maximum material removal attained in the combination of 1850 rpm, 0.6 mm, 1500 mm/min, and 8 l/min
- (4) All the above cases stand valid till they are treated as single responses.
- (5) In multiobjective optimization, the optimum level is achieved at 2495.75 rpm, 0.47 mm, 1000 mm/min, and 8 l/min using Box-Behnken design
- (6) In GRA, better results are attained at 2500 rpm, 0.2 mm, 1500 mm/min, and 6 l/min
- (7) Since the percentage deviation is within 10% both optimization techniques can be considered for machining of the investigated material.

Data Availability

The data used to support the findings of this study are included within the article.

Disclosure

This study was performed as a part of the employment of Addis Ababa Science and Technology University, Ethiopia.

Conflicts of Interest

The authors declare that there are no conflicts of interest regarding the publication of this article.

References

- [1] W. Ming-Yung and H.-Y. Chang, "Experimental study of surface roughness by the slot end milling AL2014-T6," *International Journal of Machine Tools and Manufacture*, vol. 44, pp. 51–57, 2004.
- [2] P. Palanisamy, I. Rajendran, and S. Shanmugasundaram, "Optimization of machining parameters using genetic algorithm and experimental validation for end-milling operations," *International Journal of Advanced Manufacturing Technology*, vol. 32, no. 7–8, pp. 644–655, 2007.
- [3] R. Suresh Kumar, V. S. Thangarasu, and S. John Alexis, "Adaptive control systems in CNC machining processes—a review," *Advances in Natural and Applied Sciences*, vol. 10, no. 6, pp. 120–129, 2016.
- [4] M. E. Martellotti, "An analysis of the milling process," *Trans ASME*, vol. 63, p. 667, 1941.
- [5] G. Quintana, J. d. Ciurana, and J. Ribatallada, "Surface roughness generation and material removal rate in ball end milling operations," *Materials and Manufacturing Processes*, vol. 25, no. 6, pp. 386–398, 2010.
- [6] A. Mansour and H. Abdalla, "Surface roughness model for end milling: a semi-free cutting carbon casehardening steel (EN 32) in dry condition," *Journal of Materials Processing Technology*, vol. 124, no. 1–2, pp. 183–191, 2002.
- [7] R. Suresh Kumar, K. P. Dhanabalakrishnan, and S. John Alexis, "Application of GA & ANN for the optimization of cutting parameters for end milling operations—a comparison," *International Journal of Applied Engineering Research*, vol. 10, no. 20, pp. 18092–18107, 2015.
- [8] M. Alauddin, M. A. El Baradie, and M. S. J. Hashmi, "Prediction of tool life in end milling by response surface methodology," *Journal of Materials Processing Technology*, vol. 71, no. 3, pp. 456–465, 1997.
- [9] H.-K. Chang, J.-H. Kim, I. H. Kim, D. Y. Jang, and D. C. Han, "In-process surface roughness prediction using displacement signals from spindle motion," *International Journal of Machine Tools and Manufacture*, vol. 47, no. 6, pp. 1021–1026, 2007.
- [10] S. A. Coker and Y. C. Shin, "In-process control of surface roughness due to tool wear using a new ultrasonic system," *International Journal of Machine Tools and Manufacture*, vol. 36, no. 3, pp. 411–422, 1996.
- [11] C. Gologlu and N. Sakarya, "The effects of cutter path strategies on surface roughness of pocket milling of 1.2738 steel based on Taguchi method," *Journal of Materials Processing Technology*, vol. 206, no. 1–3, pp. 7–15, 2008.
- [12] V. G. Dhokia, S. Kumar, P. Vichare, and S. T. Newman, "An intelligent approach for the prediction of surface roughness in ball-end machining of polypropylene," *Robotics and Computer-Integrated Manufacturing*, vol. 24, no. 6, pp. 835–842, 2008.
- [13] R. Suresh Kumar, V. S. Thangarasu, and S. John Alexis, "Optimization of high speed CNC end milling process of BSL 168 aluminium composite for aeronautical applications," *Transactions of the Canadian Society for Mechanical Engineering*, vol. 41, no. 4, pp. 609–625, 2018.
- [14] S.-J. Lou and J. C. Chen, "In-process surface roughness recognition (ISRR) system in end-milling operations," *International Journal of Advanced Manufacturing Technology*, vol. 15, no. 3, pp. 200–209, 1999.
- [15] Y.-H. Tsai, J. C. Chen, and S.-J. Lou, "An in-process surface recognition system based on neural networks in end milling cutting operations," *International Journal of Machine Tools and Manufacture*, vol. 39, no. 4, pp. 583–605, 1999.
- [16] P. G. Benardos and G. C. Vosniakos, "Prediction of surface roughness in CNC face milling using neural networks and Taguchi's design of experiments," *Robotics and Computer-Integrated Manufacturing*, vol. 18, no. 5–6, pp. 343–354, 2002.
- [17] C. Brecher, G. Quintana, T. Rudolf, and J. Ciurana, "Use of NC kernel data for surface roughness monitoring in milling operations," *International Journal of Advanced Manufacturing Technology*, vol. 53, no. 9–12, pp. 953–962, 2011.
- [18] J. C. Chen and M. S. Lou, "Fuzzy-nets based approach to using an accelerometer for an in-process surface roughness prediction system in milling operations," *International Journal of Computer Integrated Manufacturing*, vol. 13, no. 4, pp. 358–368, 2000.
- [19] Y. M. Ali and L. C. Zhang, "Surface roughness prediction of ground components using a fuzzy logic approach," *Journal of Materials Processing Technology*, vol. 89–90, no. 90, pp. 561–568, 1999.
- [20] S. R. Kumar, J. S. Alexis, and V. S. Thangarasu, "Experimental investigation of influential parameters in high speed machining of AMS 4205," *Asian Journal of Research in Social Sciences and Humanities*, vol. 7, no. 2, pp. 508–523, 2017.
- [21] A. M. Zain, H. Haron, and S. Sharif, "An overview of GA technique for surface roughness optimization in milling process," in *Proceedings of the IEEE International Symposium On Information Technology*, vol. 4, pp. 1–6, Kuala Lumpur, Malaysia, August 2008.
- [22] R. Suresh Kumar, V. S. Thangarasu, and S. John Alexis, "Prediction of machining parameters for A91060 in end milling," *Advances in Natural and Applied Sciences*, vol. 10, no. 6, pp. 157–163, 2016.
- [23] M. Brezocnik and M. Kovacic, "Integrated genetic programming and genetic algorithm approach to predict surface roughness," *Materials and Manufacturing Processes*, vol. 18, no. 3, pp. 475–491, 2003.
- [24] S. Ganesh Kumar, R. Suresh Kumar, Y. Suresh Babu, and Balasubramani, "A review on cutting tool measurement in turning tools by cloud computing systems in industry 4.0 and IoT," *GIS Science Journal*, vol. 7, no. 8, pp. 1–7, 2020.
- [25] H. Oktem, T. Erzurumlu, and F. Erzincanlı, "Prediction of minimum surface roughness in end milling mold parts using neural network and genetic algorithm," *Materials & Design*, vol. 27, no. 9, pp. 735–744, 2006.
- [26] S. Venkatesh, R. Suresh Kumar, S. P. Sivapirakasam, M. Sakthivel, D. Venkatesh, and S. Yasar Arafath, "Multi-objective optimization, experimental and CFD approach for performance analysis in square cyclone separator," *Powder Technology*, vol. 371, pp. 115–129, 2020.
- [27] S. Ganesh Kumar, R. Suresh Kumar, Y. Suresh Babu, and Balasubramani, "A numerical approach to cutting tool stress in CNC turning of EN8 steel with silicon carbide tool insert," *International Journal of Scientific & Technology Research*, vol. 8, no. 12, pp. 3227–3231, 2019.